Nanoscale

Accepted Manuscript

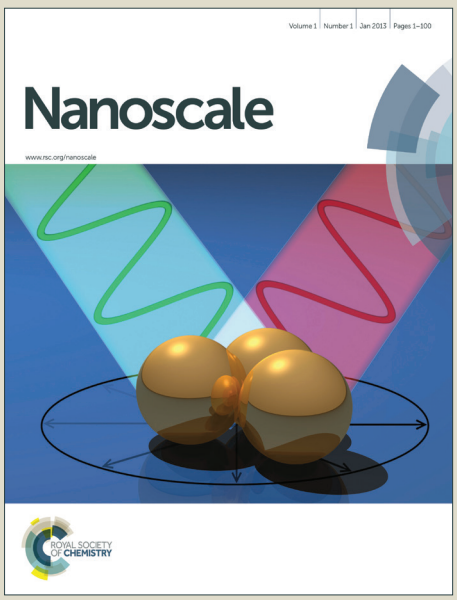

ROYAL SOCIETY OF CHEMISTRY

www.rsc.org/nanoscale

ARTICLE TYPE www.rsc.org/xxxxxx | XXXXXXXX

Synthesis of FeCo nanocrystals encapsulated in nitrogen-doped graphene layers as highly efficient catalysts for reduction reactions

Lin Hu,[‡a] Ruirui Zhang,[‡b] Lingzhi Wei,[a] Fapei Zhang,[a] and Qianwang Chen*[ab]

Received (in XXX, XXX) Xth XXXXXXXXX 200X, Accepted Xth XXXXXXXXX 200X
First published on the web Xth XXXXXXXXX 200X
DOI: 10.1039/b000000x

A facile strategy has been designed to fabricate FeCo nanocrystals with nitrogen-doped graphene shells, which involves the one-step thermal decomposition of Prussian Blue Analogue (PBA) $Fe_3[Co(CN)_6]_2$ spheres. The as-prepared product can be used as a non-precious metal catalyst with highly efficient catalytic activity and magnetic separable capability in reduction of 4-nitrophenol.

Magnetic micro/nanostructures have attracted intensive interests because of their excellent physical, catalytic, and magnetic properties and their crucial applications in diverse fields, including high-density magnetic storage devices, magnetic resonance imaging, magnetic fluids, magnetic sensors, catalyst, environmental remediation, and biological applications.[1-6] As one of important magnetic metal alloys, FeCo nanocrystals have superior magnetic properties. However, the problems of easy oxidation and potential toxicity have impeded its wide applications. Therefore, it is necessary to coat FeCo nanocrystals with air-stable materials for their practical applications. It is well known that carbon is one of the best solutions for encapsulation because of its biocompatibility and chemical stability. For example, Nano-Fe^0 encapsulated in microcarbon spheres not only leads to high performance, but also good stability.[7] Previously, FeCo nanocrystals with multilayered graphitic carbon, pyrolytic carbon, carbon nanotubes or inert metals have been obtained.[1,8-10] For example, Dai et al reported FeCo/graphitic-shell nanocrystals as advanced magnetic-resonance-imaging and near-infrared agents.[1] However, so far, there is few record on the formation of FeCo nanocrystals with nitrogen-doped graphene layers by a simple one-step strategy.

Metal-organic frameworks (MOFs) contain metal ions linked by coordinated ligands, which is described as a new class of porous materials. Previous studies have demonstrated that MOFs can act as both templates and precursors for the preparation of porous materials.[11-17] Our group demonstrated that the hollow/porous oxides could be obtained by the calcination of nanoscale MOFs in air.[18-21] As we know, nitrogen-doped carbon materials often exhibit excellent performance for various applications.[22-23] It is worth mentioning that nitrogen-doped porous carbon materials also have been obtained by choosing the nitrogen containing MOFs as precursors, such as ZIFs.[24] Xu and co-workers reported the first example of the synthesis of porous carbon materials using a nitrogen containing MOF as the precursor.[25] Recently, Yusuke Yamauchi et al reported the formation of nanoporous carbon with magnetic Co nanoparticles towards excellent adsorption of methylene blue by one-step carbonization of zeolitic imidazolate framework-67 crystals.[26] $Fe_3[Co(CN)_6]_2$ is one of typical Prussian Blue Analogues (PBA), which is rich in carbon, nitrogen, iron and cobalt, may be an ideal precursor for the synthesis nitrogen-doped carbon with magnetic alloys. Here, we report a facile synthesis of FeCo nanocrystals encapsulated in nitrogen-doped graphene layers by the simple annealing of $Fe_3[Co(CN)_6]_2$ spheres in nitrogen atmosphere (Scheme 1).

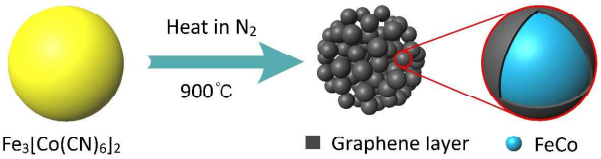

Scheme 1. Illustration of synthesis of FeCo nanocrystals with graphene layers by direct carbonization of $Fe_3[Co(CN)_6]_2$ spheres.

$Fe_3[Co(CN)_6]_2$ spheres were obtained at room temperature by simple mixing of $K_3[Co(CN)_6]$ and $FeSO_4$ in the presence of polyvinylpyrrolidone (PVP), which turn out to be in good dispersity with a large amount of spherical-like particles (Fig. S1). Without PVP, the $Fe_3[Co(CN)_6]_2$ particles are agglomerated (Fig. S2). Thermogravimetric analysis (TGA) of $Fe_3[Co(CN)_6]_2$ spheres in nitrogen atmosphere indicates three decomposition steps (Fig. S3). The first shows a sharp weight loss from room temperature to 132 ◦C illustrating the loss of water molecules from the porous structure. The second step is observed due to the collapse of framework to form the product. The third step may be attributed to the loss of nitrogen element at high temperature.[24a] The obtained $Fe_3[Co(CN)_6]_2$ powders were directly carbonized under a nitrogen flow at 900 °C based on the thermogravimetry results. Scanning electron microscopy (SEM), transmission electron microscopy (TEM), X-ray diffraction (XRD) and X-ray photoelectron spectroscopy (XPS) were employed to characterize the obtained product. Fig. 1a shows the typical SEM image of the product, which displays large-scale particles. The high-magnification SEM image (Fig. 1b) reveals that the particles also turn out to be spherical-like and the surfaces are very rough. Due to the shrinkage at high temperature, the size of the particles appears to be smaller, compared to that of $Fe_3[Co(CN)_6]_2$. The TEM measurement further reveals that the particles composed of carbon and smaller nanocrystals (Fig. 1c). In addition to the particles, the transparent graphene-like nanosheets are also clearly identified, as shown by the arrows in Fig. 1c. The phase of product was confirmed by XRD (Fig. 1d), which shows the

characteristic peaks at 44.8° and 65.3°, corresponding to the (110) and (200) planes of the FeCo alloy (JCPDS 49-1567), respectively. No peaks of impurities can be detected from this pattern. Based on Scherrer formula ($D=0.89\lambda/B\cos\theta$), an average crystalline size of 46 nm is estimated from (110) peak (the strongest peak). As shown from Fig. S4, it can be observed the product displays three Raman peaks centered at around 1348 cm^{-1}, 1595 cm^{-1} and 2700 cm^{-1}, which correspond to the D, G and 2D bands, respectively. High-resolution TEM image of single nanocrystal clearly shows that the nanocrystal is completely coated by the shells with a interlayer distance of 3.41 Å (Fig. 2a and Fig. S5). The box section in Fig. 2a reveals that the thickness of shell is 5 layers, which indicates the existence of graphene layer. The FeCo nanocrystal exhibits a d-spacing of 2.02 Å (the inset in Fig. 2a), corresponding to the (110) plane of the FeCo alloy. The EDS spectrum of single FeCo nanocrystal reveals that the molar ratio of Fe and Co is close to 3:2, which is similar to the ratio in $Fe_3[Co(CN)_6]_2$ (Fig. 2b). The typical XPS spectra of the product show the presence of O, C, N, Fe and Co (Fig. S6). It should be noted that the surface Fe and Co contents is only 2.03 and 1.68 at.%, respectively, which is lower than that in $Fe_3[Co(CN)_6]_2$. This XPS result further indicates that the FeCo nanocrystals are almost fully confined in the interior of graphene shells. It is worth mentioning that the N and C content in the product are 3.79 and 86.58 at.%, respectively. The N1s spectrum (the inset in Fig. 2b) can be deconvoluted to five individual peaks that are assigned to pyridinic N (398.9 eV), pyrrolic N (400.1, 400.6 eV), and quaternary N (401.2, 402.1 eV).[27] Fig. 3b-f shows STEM-energy dispersive X-ray (STEM-EDX) elemental mapping of Fe, Co, C, N and O, respectively. The uniform distribution of oxygen is attributed to the adsorption of air due to the relative high surface area and pores of the shells (Fig. S7 and S8). Fig. S9 displays TGA profiles of the product under air. The weight loss below 100 °C is attributed to desorption of air, while weight change from 200°C to 450 °C is attributed to the combustion of graphene layers and oxidation of FeCo nanocrystals, indicating the good stability below 200°C.

Actually, there is a general strategy to synthesize magnetic nanoparticles with nitrogen-doped carbon shells by one-step thermal decomposition of Prussian blue and its analogue.[17] For example, Fe/Fe_3C nanoparticles with nitrogen-doped carbon shell has been successfully synthesized via the direct pyrolysis of Prussian blue (PB) nanocubes (Fig. S10 and S11).

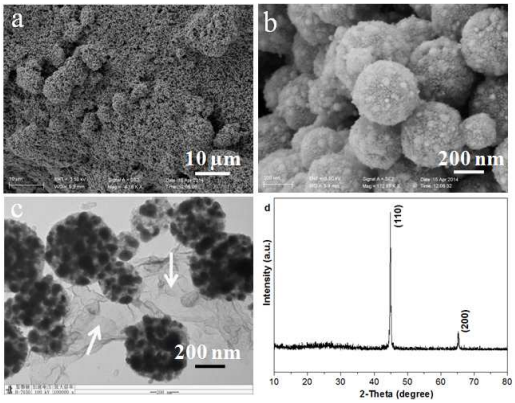

Fig. 1 (a-b) the SEM images of as-prepared product, (c) the TEM image of as-prepared product, (d) the XRD pattern of as-prepared product.

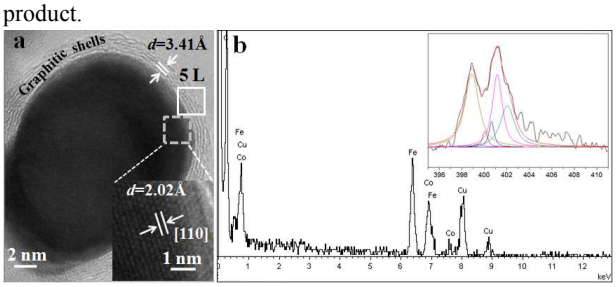

Fig. 2 (a) The HRTEM image of single FeCo nanocrystal (b) The EDS spectrum of single FeCo nanocrystal. The inset is the high resolution XPS spectra of N1s.

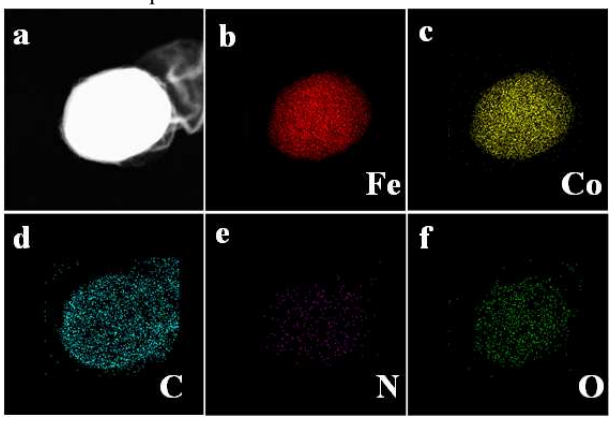

Fig. 3(a) Dark-field STEM image of single FeCo nanocrystal.(b-f)Elemental mapping of the same nanocrystal, indicating the spatial distribution of Fe (b), Co (c), C (d), N(e) and O (f) respectively.

4-nitrophenol (4-NP) is considered to be one of the most prevalent organic pollutants in waste-waters generated from agricultural and industrial sources, and the nitro to amino conversion has great industrial relevance such as for aniline and paracetamol production. In previous studies, noble metals are a commonly used and efficient catalyst, but the high cost limits their applications, especially for large-scale systems.[28] Recently, nitrogen-doped graphene also has been employed as a catalyst for 4-NP reduction reaction by our group.[29-30] All four kinds of the doped nitrogen atoms are beneficial to the adsorption and activation of 4-NP, contributing to the catalytic reduction reaction. However, the catalyst only can be separated from reaction system for repeated use by centrifuging (8000 rpm, 30 min), which is not consistent with the criterion of energy conservation. In this regards, magnetically functionalized nitrogen-doped carbon materials have entered into our sight because of the easy separation. It is interesting to test the catalytic activity of FeCo nanocrystals with nitrogen-doped graphene shells as a non-precious metal catalyst for reduction of 4-NP in water. It is well known FeCo alloy possesses excellent magnetic properties, which enables them to be recycled easily from the solution with the help of an external magnetic field. Fig. S12 shows the *M–H* hysteresis loop of product measured at room temperature (300K). The saturation magnetization value *Ms* for the product is 154 emu g^{-1}. And the coercivity value *Hc* is 430 Oe. The quick response of FeCo nanocrystals to the external magnetic field was

demonstrated by placing a magnet near the vessel after the finish of reaction (the inset in Fig. 4a). Moreover, the graphene shells not only could prevent the direct contact between FeCo nanocrystals and treated solutions to avoid the further pollution, but also ensure the stability in an acidic/alkaline environment to some extent.

The reduction of 4-NP by $NaBH_4$ was employed as the model reaction to determine the catalytic ability of the as-prepared product at room temperature. It is observed that the intensity of the characteristic absorption peak of 4-NP at 400 nm quickly decreases, and the characteristic absorption of 4-aminophenol (4-AP) at around 303 nm also appears rapidly (Fig. 4a). This indicates that 4-NP is reduced to 4-AP quickly with discoloration of the solution from bright yellow to colorless (the inset in Fig.4a). It should be noted that the completion time was only 321s after adding the catalyst. The time dependent absorptions at 400 nm were also recorded. The estimated completion time of as-prepared FeCo nanocrystals was about 350s (Fig. 4b). Fig. 4c shows $\ln(C/C_0)$ versus reaction time for the reduction of 4-NP over the as-prepared FeCo nanocrystals. The kinetic constant k_{app} was 8.28×10^{-3} s^{-1} (0.4968 min^{-1}) according to the slope of the fitted line. It is worth mentioning that the k_{app} value is comparable to that of some precious metal catalysts for reduction 4-NP, such as Fe_3O_4@TiO_2/Au@SiO_2/Pd microsphere (0.23887 min^{-1}),[28e] Pd@Au core-shell nanotetrapod (0.139 min^{-1}),[28f] Pd/C (8.83×10^{-3} s^{-1}).[28g] Moreover, the k_{app} value is much higher than that of $NiCo_2$ alloy (0.07348 min^{-1}).[4] The completion time (6 min) is much lower than that of metal-free nitrogen-doped graphene catalyst (21 min).[29] The excellent catalytic activity of as-prepared FeCo nanocrytals may originate from the following reasons: (i) The synergistic effect of FeCo nanocrystals and nitrogen-doped graphene shells. (ii) The relatively small size of FeCo nanocrystals. It deduces that not only FeCo nanocryatals, but also the nitrogen-doped graphene shell contribute to the catalytic effect based on previous results.[29] Recently, Au-Cu alloy nanocrystals exhibited excellent catalytic activity for reduction of 4-NP owing to the synergistic effect of the two metal components.[31] In this regards, it is believed that the synergistic effect of Fe and Co components could enhance the catalytic activity. Indeed, under the same experimental condition, the completion time (538s) under Fe/Fe_3C nanocrystals is longer than that of FeCo nanocrystals (321s), as shown from Fig. S13. Moreover, due to the release of gas during thermal decomposition process, the obtained graphene shells possess pores which will connect with each other to form inter-connected channels (active pores) that allow the reactants to be transported through the catalyst. The doped nitrogen not only introduces active sites, but also improves the adsorption ability of graphene layer for 4-NP ions, which will contribute to the catalytic properties.[29] It is well known that the surface area to volume ratio dramatically increases as the size of nanoparticles decrease, so the relative small-sized FeCo nanoparticles greatly improve the utilization efficiency of FeCo alloy.

The reusable catalytic properties of as-prepared FeCo nanocrystals are shown in Fig. 4d. The conversion of 4-NP can achieve above 95% even after running for ten cycles, indicating stable catalytic performance. Moreover, the XRD pattern of FeCo nanocrystals after ten catalytic cycles has been measured (Fig. S14). Also, no peaks of impurities can be detected from this pattern, indicating the chemical stability of FeCo nanocrystals. TEM image clearly shows the spherical-like particle and shell (Fig. S15), indicating the good structural stability.

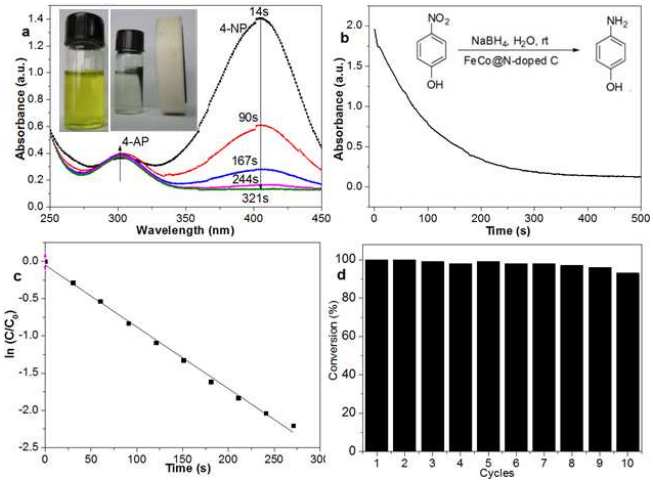

Fig. 4 (a) UV-vis spectra of solutions of 4-NP sampled at different reaction durations. (b) Time dependence of the absorption of 4-NP at 400 nm. (c) Plots of ln (C_t/C_0) of 4-NP versus reaction time. (d) The catalytic stability tests of product.

In summary, FeCo nanocrystals with nitrogen-doped graphene layers were obtained by the thermal decomposition of $Fe_3[Co(CN)_6]_2$ spheres. The synthesized FeCo nanocrystals show a strong magnetic response. When employed as a catalyst for reduction of 4-NP, the FeCo nanocrystals not only exhibit high catalytic activity and stability due to their structural features, but also can be separated easily with the help of a magnet. The k_{app} value is comparable to that of some precious metal catalysts for reduction 4-NP. As we know, the graphene-encapsulated metal catalyst, on which O_2 is readily activated by the electrons transferred from the metal to the surface, has been demonstrated as a promising strategy to produce robust non-precious metal electrocatalysts. Therefore, it is expected that FeCo nanocrytstals with nitrogen-doped graphene shells exhibit excellent catalytic activity towards a wide range of reactions, such as the oxygen reduction reaction.[2] By changing the metal ions in MOFs, we believe that series of metals or alloys with carbon or graphene shells will be obtained.

This work was supported by the National Natural Science Foundation (NSFC 21271163, U1232211, 21301178) and the China Postdoctoral Science Foundation (2012M521261).

Notes and references

[a] *High Magnetic Field Laboratory, Hefei Institutes of Physical Science; Chinese Academy of Sciences, Hefei, Anhui, 230031, P. R. China*

[b] *Division of Nanomaterials and Chemistry, Hefei National Laboratory for Physical Sciences at the Microscale, Department of Materials Science and Engineering, University of Science*

and Technology of China, Hefei, 230026, P.R. China,
Fax: + 86-551-63603005 Tel: + 86-551-63603005;
E-mail: cqw@ustc.edu.cn.

† Electronic Supplementary Information (ESI) available: Experimental details and characterization: Fig.S1-Fig.S15. See DOI: 10.1039/b000000x/

‡These authors contributed equally to this work.

1 W. S. Seo, J. H. Lee, X. M. Sun, Y. Suzuki, D. Mann, Z. Liu, M. Terashima, P. C. Yang, M. V. Mcconnell, D. G. Nishimurai and H. J. Dai, *Nat. Mater*., 2006, **5**, 971.

2 G. Wu, K. L. More, C. M. Johnston and P. Zelenay, *Science*, 2011, **332**, 443.

3 D. H. Liu, Y. Guo, L. H. Zhang, W. C. Li, T. Sun and A. H. Lu, *Small*, 2013, **9**, 3852.

4 K. L. Wu, X. W. Wei, X. M. Zhou, D. H. Wu, X. W. Liu, Y. Ye and Q. Wang, *J. Phys. Chem. C*, 2011, **115**, 16268.

5 A. A. EI-Gendy, E. M. M. Ibrahim, V. O. Khavrus, Y. Krupskaya, S. Hample, A. Leonhardt, B. Büchner and R. Klingeler, *Carbon*, 2009, **47**, 2821.

6 C. Singh, A. Goyal and S. Singhal, *nanoscale* 2014, **6**, 7959.

7 H. Q. Sun, G. L. Zhou, S. Z. Liu, H. M. Ang, M. O. Tadé and S. B. Wang, *ACS Appl. Mater. Interfaces*., 2012, **4**, 6235.

8 C. Desvaux, C. Amiens, P. Fejes, P. Renaud, M. Respaud, P. Lecante, E. Snoeck and B. Chaudret, *Nat. Mater.*, 2005, **4**, 750.

9 J. Bai and J. P. Wang, *Appl. Phys. Lett.*, 2005, **87**, 152502.

10 J. Deng, L. Yu, D. H. Deng, X. Q. Chen, F. Yang and X. H. Bao, *J. Mater. Chem. A*., 2013, **1**, 14868.

11 J. K. Sun and Q. Xu, *Energy Environ. Sci*., 2014, **7**, 2071.

12 A. J. Amali, J. K. Sun and Q. Xu, *Chem. Commun.,* 2014, **50**, 1519.

13 W. Chaikittisilp, K. Ariga and Y. Yamauchi, *J. Mater. Chem. A*, 2013, **1**, 14.

14 M. Hu, A. A. Belik, M. Imura, K. Mibu, Y. Tsujimoto and Y. Yamauchi, *Chem. Mater*., 2012, **24**, 2698.

15 L. Zhang, H. B. Wu, S. Madhavi, H. H. Hng and X. W. Lou, *J. Am. Chem. Soc*., 2012, **134**, 17388.

16 L. Zhang, H. B. Wu and X. W. Lou, *J. Am. Chem. Soc*., 2013, **135**, 10664.

17 X. J. Zheng, J. Deng, N. Wang, D. H. Deng, W. H. Zhang, X. H. Bao and C. Li. *Angew. Chem. Int. Ed*., 2014, **53**, 7023.

18 L. Hu, N. Yan, Q. W. Chen, P. Zhang, H. Zhong, X. R. Zheng, Y. Li and X. Y. Hu, *Chem*. *Eur*. *J*., 2012, **18**, 8971.

19 L. Hu, P. Zhang, H. Zhong, X. R. Zheng, N. Yan and Q. W. Chen, *Chem*. *Eur*. *J*., 2012, **18**, 15049.

20 L. Hu, Y. M. Huang, F. P. Zhang and Q. W. Chen, *Nanoscale*, 2013, **5**, 4186.

21 L. Hu and Q. W. Chen, *Nanoscale*, 2014, **6**, 1236.

22 H. Q. Sun, Y. X. Wang, S. Z. Liu, L. Ge, L. Wang, Z. H. Zhu and S. B. Wang, *Chem. Commun*., 2013, **49**, 9914.

23 Y. Y. Jiang, Y. Z. Lu, X. D. Wang, Y. Bao, W. Chen and L. Niu, *Nanoscale*, DOI: 10.1039/c4nr04295f.

24 (a) L. J. Zhang, Z. X. Su, F. L. Jiang, L. L. Yang, J. J. Qian, Y. F. Zhou, W. M. Li and M. C. Hong, *Nanoscale*, 2014, **6**, 6590; (b) R. Li, X. Q. Ren, X. Feng, X. G. Li, C. W. Hu and B. Wang, *Chem. Commun*., 2014, **50**, 6894; (c) P. P. Su, H. Xiao, J. Zhao, Y. Yao, Z. G. Shao, C. Li and Q. H. Yang, *Chem. Sci*., 2013, 4, 2941.

25 H. L. Jiang, B. Liu, Y. Q. Lan, K. Kuratani, T. Akita, H. Shioyama, F. Q. Zong and Q. Xu, *J. Am. Chem. Soc*., 2011, **133**, 11854.

26 N. L. Torad, M. Hu, S. Ishihara, H. Sukegawa, A. A. Belik, M. Imura, K. Ariga, Y. Sakka and Y. Yamauchi, *Small*, 2014, **10**, 2096.

27 H. B. Wang, T. Maiyalagan and X. Wang, *ACS Catal*., 2012, **2**, 781.

28 (a) J. Zeng, Q. Zhang, J. Y. Chen and Y. N. Xia, *Nano Lett.*, 2010, **10**, 30; (b) B. J. Lee, J. C. Park and H. Song, *Adv. Mater*., 2008, **20**, 1523; (c) X. Q. Huang, C. Y. Guo, J. Q. Zuo, N. F. Zheng and G. D. Stucky, *Small*, 2009, **5**, 361; (d) T. Yu, J. Zeng, B. Lim and Y. N. Xia, *Adv. Mater.*, 2010, **22**, 5188; (e) W. T. Hu, B. C. Liu, Q. Wang, Y. Liu, Y. X. Liu, P. Jing, S. L. Yu, L. X. Liu and J. Zhang, *Chem. Commun*., 2013, **49**, 7596; (f) R. P. Zhao, M. X. Gong, H. M. Zhu, Y. Chen, Y. W. Tang and T. H. Lu, *Nanoscale*, DOI:10.1039/C4NR02214A; (g) Y. X. Fang and E. K. Wang, *Nanoscale*, 2013, **5**, 1843.

29 X. K. Kong, Z. Y. Sun, M. Chen, C. L. Chen and Q. W. Chen, *Energy Environ. Sci.*, 2013, **6**, 3260.

30 X. K. Kong, C. L. Chen and Q. W. Chen, *Chem. Soc. Rev.*, 2014, **43**, 2841.

31 R. He, Y. C. Wang, X. Y. Wang, Z. T. Wang, G. Liu, W. Zhou, L. P. Wen, Q. X. Li, X. P. Wang, X. Y. Chen, J. Zeng and J. G. Hou, *Nat. Commun*., 2014, **5**, 4327.